

# Electromagnetic properties and He<sup>+</sup> irradiation effects on YBa<sub>2</sub>Cu<sub>3</sub>O<sub>7-x</sub> grain-boundary Josephson junctions

M. A. Navacerrada, M. L. Lucía, and F. Sánchez-Quesada

*Departamento de Física Aplicada III, Facultad de Ciencias Físicas, Universidad Complutense de Madrid, Avda. Complutense s/n. 28040 Madrid, Spain*

(Received 3 March 1999; revised manuscript received 23 April 1999)

We have analyzed the electromagnetic properties of small and long YBa<sub>2</sub>Cu<sub>3</sub>O<sub>7-x</sub> grain-boundary Josephson junctions. The Swihart velocity increases with junction width ( $w$ ) while the ratio of the relative dielectric constant to the barrier thickness ( $\epsilon/t$ ) decreases. We found that the product  $w \times \epsilon/t$  is approximately constant. These results have been explained in the framework of the filamentary model, where the barrier can be regarded as a disordered dielectric medium with a high density of superconducting filaments. Experiments demonstrate that a controllable variation of these parameters can be achieved by helium irradiation at 80 keV. We give examples of an enhancement of weak-link properties of junctions for doses in the range of  $10^{13}$  cm<sup>-2</sup>. Raising the dose we can sweep the modification of the weak-link properties from an increase of the junction critical current of about 10% to a severe degradation of the coupling energy of the barrier, although the superconducting properties of the electrodes always worsen gradually.

## I. INTRODUCTION

Josephson junctions play a key role in electronic devices.<sup>1</sup> Control and reproducibility of the properties of high-temperature superconductor Josephson junctions is essential for the development of new electronics. In this recent technological area, a widely used technique for the fabrication of high-temperature junctions is the epitaxial growth of YBa<sub>2</sub>Cu<sub>3</sub>O<sub>7-x</sub> (YBCO) on bicrystalline substrates with one tilt grain boundary. The nature of the weak link at the grain-boundary junctions (GBJ's) generated in the YBCO layer grown on top is still controversial.<sup>2,3</sup> Moreover, it is well known that the grain boundaries are extremely sensitive to the growth parameters<sup>4,5</sup> provided that film growth takes place in conditions far from equilibrium. Among the different models proposed to explain the properties of YBCO GBJ's the filamentary model<sup>6</sup> is frequently referred. Comparative electromigration studies between grain-aligned microbridges and microbridges containing high-angle tilt boundaries suggest that the initial effect of a grain boundary is to exacerbate the disorder in the adjacent regions. On the basis of these observations, this phenomenological model analyzes the grain boundaries bridged by an array of superconductive connections and by another array of normal paths that do not carry supercurrent. This model is consistent with a wide set of experimental results. The model explains satisfactorily the half-integral constant voltage steps observed in many grain-boundary Josephson junctions.<sup>7</sup> Photoexcitation experiments give evidence of the existence of regions with substantial oxygen deficiency and/or disorder near the grain boundary.<sup>8</sup> High-resolution<sup>5,9</sup> microscopy images show that low-angle grain boundaries are composed of arrays of dislocations. The strain fields of dislocations perturb the local electronic structure leading to a nonsuperconducting zone at the grain boundary. Therefore the supercurrent flows predominantly through channels of good crystalline lattice order between dislocations.<sup>10,11</sup> High-angle grain boundaries can-

not be described by this model since dislocation cores may overlap; however, strongly coupled paths have also been demonstrated in this case, so that the filamentary model has been generalized.<sup>12</sup>

An important tool for understanding the microstructure and nature of the grain boundary is the study of critical current ( $I_C$ ) spatial distribution in GBJ's. Some studies in small junctions using the inverse Fourier transform on critical current versus magnetic field dependence,  $I_C(B)$ , give clear evidence that  $I_C$  has spatial inhomogeneities on a length scale down to 1 nm.<sup>13,14</sup> Analytical and numerical studies have been developed in long Josephson junctions, solving the static sine-Gordon equation, in the presence of different types of structural disorder.<sup>15</sup> In any case the literature presents an excessive variation of critical parameters such as  $I_C$  and junction resistance ( $R_N$ ) for all junction types, even in the same chip. Only a few empirical conclusions and relations are frequently reported for GBJ's: for instance, a stronger coupling behavior for lower-tilt angle boundaries,<sup>3,10</sup> and a scaling behavior for the characteristic voltage  $V_C = I_C R_N$ , which is proportional to  $(J_C)^{q/q+1}$  with  $q \approx 1.5$ , where  $J_C$  is the critical current density, when bicrystalline SrTiO<sub>3</sub> substrates are used.<sup>16</sup> In this framework, several experiments have been developed to study the possibility of adjusting the barrier parameters *a posteriori*. In junctions made on bicrystals, the critical current  $I_C$  increases and the normal resistance  $R_N$  decreases after an annealing treatment in ozone.<sup>17</sup> Recently, Ca-doping of YBCO films has also provided a way to increase  $I_C$  and to reduce significantly  $R_N$  of GBJ's.<sup>18,19</sup> On the contrary, a controlled worsening of these parameters is observed when the barrier is modified by electron beam<sup>20</sup> and proton irradiation.<sup>21</sup> However, none of these last studies have been done on GBJ's made on bicrystals.

In this paper we present a detailed revision of the most important parameters that can be deduced from transport measurements,  $I_C(B)$  and current-voltage ( $I-V$ ) characteristics, on YBCO Josephson junctions grown on bicrystalline

substrates. We present a separated analysis of the transport ( $I_C, R_N$ ) and electromagnetic (Swihart velocity and dielectric constant) parameters of the barrier, and in both cases the results can be explained in the context of the filamentary model. We also demonstrate for the first time to our knowledge that ion bombardment of the junctions can enhance  $I_C$ : in particular, we have studied the effect of low-energy helium irradiation with variable doses.

## II. EXPERIMENT

Josephson junctions were generated using bicrystalline substrates of SrTiO<sub>3</sub> with a symmetrical tilt angle of 24°. YBCO films having 500 Å thickness and *c*-axis orientation were epitaxially grown in a high pressure (3.4 mbar) pure oxygen dc sputtering system.<sup>22</sup> In the deposition process the substrate temperature is 900 °C. Electrodes had transition temperatures ( $T_C$ ) in the range 89.5–91 K, transition widths smaller than 0.2 K and critical currents densities higher than 10<sup>6</sup> A/cm<sup>2</sup> at 77 K. Films were patterned by wet etching in H<sub>3</sub>PO<sub>4</sub>, obtaining junctions widths ranging between 2 and 50 μm. Patterned microbridges (barriers and electrodes) were irradiated at room temperature with 80 keV He<sup>+</sup> ions incident 7° from the surface normal to avoid channelling effect. Doses ranged between 5 × 10<sup>13</sup> and 5 × 10<sup>14</sup> cm<sup>-2</sup>. For this energy a projected range of 3500 Å was estimated from the SRIM 96 software, such that ions are assumed to pass through the film into the substrate where they are implanted causing the biggest damage. Ion current was kept small, in the order of 500 nA, to avoid heating of the sample during irradiation.

All electrical measurements were made in a double Co-Netic cylinder surrounding the samples for correct magnetic shielding. Curves of temperature dependence of the resistance,  $R(T)$ , were measured using a four-point configuration. The  $I$ - $V$  characteristics were registered using an ac Oxford Instruments electronic system [dc-superconducting quantum interference device system adapted to work with single Josephson junctions]. The magnetic field was applied parallel to the grain boundary plane. The critical current is identified as the current at which the dynamic resistance ( $dV/dI$ ) increases sharply. Defining the critical current by a voltage criterion gives similar results. When thermally activated phase slippage makes the  $I$ - $V$  curves rounded,  $I_C$  is determined by the intersection of the tangent  $(dI/dV)_{\min}$  with the current axis as explained in Ref. 23. Similar results are obtained for  $I_C$  using the Ambegaokar-Halperin analytical expression for the noise-rounded resistively shunted junction (RSJ) model  $I$ - $V$  curves.<sup>24</sup> The foot structure in the resistive transition of the junctions can also be accounted for by this model, so that a correct determination of  $R_N$  can be deduced from proper fittings of  $R(T)$ .<sup>25</sup>

## III. RESULTS AND DISCUSSION

### A. Electromagnetic and transport properties

Figure 1(a) shows the curve  $I_C(B)$  of a junction 2 μm wide with  $R_N$  of 17.5 Ω. The pattern fits very well a Fraunhofer-like  $|\sin \pi\Phi/\pi\Phi|$  function where flux focusing effects<sup>26</sup> associated to our planar geometry are taken into account by factor  $F$  in the flux density expression:  $\phi_0 = Fwd\Delta B$ ,<sup>27</sup> being  $\phi_0$  the flux quantum,  $\Delta B$  the width of

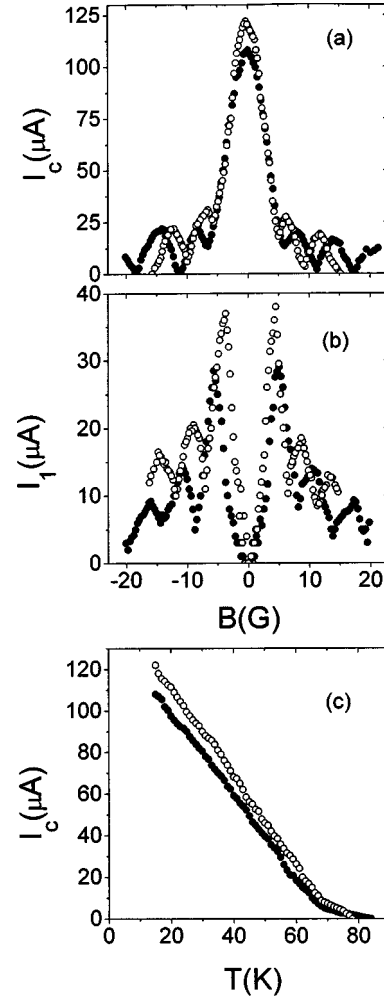


FIG. 1. Fraunhofer pattern (a), magnetic field dependence of the first Fiske step (b), and temperature dependence of critical current (c) before (black dots) and after irradiation (white dots). Dose is 5 × 10<sup>13</sup> cm<sup>-2</sup> and junction width is 2 μm. Data in (a) and (b) are measured at 15 K.

the oscillations in the  $I_C(B)$  pattern,  $w$  the width of the junction, and  $d$  the effective magnetic thickness of the junction  $d = t + 2\lambda \cong 2\lambda$  ( $t$  is the barrier thickness). In our case  $\lambda = \lambda_L \coth(\delta/\lambda_L)$  where  $\delta$  is the thickness of the films, since  $\delta$  is smaller than the London penetration depth  $\lambda_L$ .<sup>28</sup> In the calculations we use  $\lambda_L = 140$  nm at the lowest temperature.<sup>29</sup>

We have observed Fiske steps<sup>30</sup> in our small GBJ's, and both Fiske and flux-flow resonances<sup>31</sup> in the long junctions, supporting the idea of the junctions as long parallel resonators for electromagnetic waves,<sup>28</sup> where the junction barrier forms the effective dielectric medium. Figure 1(b) shows the magnetic field dependence of the first Fiske resonance, which intensity is obtained subtracting the RSJ model calculated current to the  $I$ - $V$  measured characteristics. From the position of the resonance steps it is possible to determine the Swihart velocity  $\bar{c}$  of the resonator. In the case of Fiske steps  $V_n = (n\bar{c}\phi_0/2w)$ ,<sup>30</sup> where  $n$  is the resonance number and the resonant frequency is  $f_n = V_n/\phi_0$ . For flux-flow resonances the step voltage  $V_m$  is related to the applied magnetic flux density  $B$  by  $V_m = (\phi_0\bar{c}/w\Delta B)B$ ,<sup>27</sup> where  $\Delta B$  in large junctions can only be estimated from two nearby dips in the  $I_C(B)$  curves at each temperature. For small Josephson junc-

TABLE I. Summary of transport parameters of YBCO GBJ's on SrTiO<sub>3</sub> bicrystalline substrates. Critical currents are quoted at 20 K. Data are arranged according to  $R_N$ .

$w$ ( $\mu\text{m}$ )	$R_N$ ( $\Omega$ )	$I_C$ ( $\mu\text{A}$ )	$I_C R_N$ (mV)
50	0.94	1900	1.8
6	2.8	862	2.4
30	3	880	2.6
10	3.8	776	2.9
10	4	761	3
30	4.3	550	2.3
10	4.5	530	2.4
8	4.5	545	2.4
20	4.6	500	2.3
10	4.9	400	2
10	5	445	2.2
10	5.2	475	2.4
4	7	272	1.9
4	8.5	305	2.5
2	9.5	240	2.3
2	14	151	2.1
2	15.6	127	2
2	17.5	98	1.8

tions, we obtain  $\bar{c}$  from  $V_n$  and in the case of long junctions from both  $V_n$  and  $V_m$  since both resonances appear in the  $I$ - $V$  curves. In the case of Fiske steps we always analyze the

resonance number  $n=1$ , although the second resonance can also be seen in some of our large junctions. From the value of  $\bar{c}$  it is possible to determine the ratio of the relative dielectric constant  $\epsilon$  to the barrier thickness using the expression  $\bar{c}=[c_0(t/\epsilon d)^{1/2}]$  where  $c_0$  is the velocity of light in vacuum. All the parameters obtained from our fittings are listed in Tables I and II. We have included data from other authors for comparison as will be discussed later.  $I_C(T)$  dependence is plotted in Fig. 1(c).

It is well known that YBCO film growth occurs through the nucleation of three-dimensional islands and appears to be a mainly random process. This is consistent with TEM observations,<sup>32</sup> which show the grain-boundary plane to meander or facet around the boundary direction defined by the bicrystalline substrate, avoiding any possible prediction of the exact boundary structure. Data are presented in Table I according to the values of  $R_N$ , a parameter closely related with the growth process of the film and the barrier. We have checked that the value of the critical current is mainly dependent on the value of  $R_N$ . The product  $I_C R_N$  is basically constant in our samples rather than fitted to a scaling law. In fact although Table I only shows  $I_C$  at 20 K, similar values of  $R_N$  give raise to similar  $I_C(T)$  curves. The filamentary model could account for these results. No clear correlation exists between these parameters and the width of the microbridge; junctions with different widths may have similar values of  $R_N$ . The distribution and quality of the channels in the grain boundary that carry supercurrent fix both  $R_N$  and  $I_C(T)$ . The distribution of these filaments is basically random and exclusively dependent on the growth process of the barrier.

TABLE II. Summary of electromagnetic parameters of YBCO GBJ's on SrTiO<sub>3</sub> bicrystalline substrates. Data of resonant frequency  $f_1$ , Swihart velocity  $\bar{c}$ , and ratio  $\epsilon/t$  are quoted at 20 K and arranged according to  $w$ .

$w$ ( $\mu\text{m}$ )	$\delta$ (nm)	$R_N$ ( $\Omega$ )	$f_1$ ( $\times 10^{11} \text{ s}^{-1}$ )	$\bar{c}$ ( $\times 10^6 \text{ m/s}$ )	$\epsilon/t$ ( $\text{nm}^{-1}$ )	$w \times \epsilon/t$ ( $\times 10^4$ )
50	50	0.94	0.82	8.2	1.6	8
30	50	4.3	1.06	6.4	2.6	7.8
30	50	3	1.12	6.7	2.4	7.2
30 <sup>a</sup>	200 <sup>a</sup>		1.61 <sup>a</sup>	9.7 <sup>a</sup>	3.4 <sup>a</sup>	10.2 <sup>a</sup>
20	50	4.6	1.25	5	4.4	8.8
10	50	5	1.7	3.4	9.5	9.5
10	50	4.9	1.75	3.5	8.9	8.9
10	50	4.5	1.75	3.5	8.8	8.8
10	50	5.2	1.8	3.6	8.5	8.5
10	50	4	1.9	3.8	7.5	7.5
10	50	3.8	2	4	6.8	6.8
8	50	4.5	2	3.2	10.7	8.6
6	50	2.8	2.33	2.8	14	8.4
5 <sup>b</sup>	$\approx 200-300$ <sup>b</sup>	6 <sup>b</sup>	4 <sup>b</sup>	4 <sup>b</sup>	20 <sup>b</sup>	10 <sup>b</sup>
4	50	9.5	3.1	2.5	17.3	7
4	50	8.5	3.25	2.6	16.1	6.5
2	50	9.5	4	1.6	43	8.6
2	50	17.5	4.5	1.8	33.6	6.7
2	50	15.6	5	2	27.5	5.5
2	50	14	5.75	2.3	20.7	4.2

<sup>a</sup>Reference 27.

<sup>b</sup>Reference 8.

On the other hand, the presence of resonances supports the picture of the barrier as a dielectric medium. In Table II we have now quoted  $f_1$ ,  $\bar{\tau}$ , and  $\varepsilon/t$  according to the junction width, which has shown to be the main parameter in the following discussion. The value of  $\bar{\tau}$  increases with junction width while  $\varepsilon/t$  decreases. If we compare junctions of the same width we observe that these parameters are only slightly dependent of  $R_N$ . Surprisingly  $\varepsilon/t$  increases with the resonant frequency, which is essentially fixed by the width of the resonant cavity. Thus the model for this resonator as a perfect dielectric medium is inadequate to explain this dependence. We have extended this model to  $RLC$  parallel circuit.  $R$  accounts for the transport of quasiparticles ( $R=R_N$ ) and  $C$  for the dielectric response of the barrier ( $C=\delta w \varepsilon_0 \varepsilon_r/t$ ). Because of the large magnetic penetration depth of YBCO the kinetic inductance should also be taken into account<sup>33</sup> and may be expressed as  $L=L_k \approx \frac{1}{4} \mu_0 \lambda_L [\coth(\delta/2\lambda_L) + \delta/2\lambda_L \text{sh}^2(\delta/2\lambda_L)]$ . Assuming for the relative dielectric constant  $\varepsilon_r$  the value estimated for oxygen deficient YBCO,  $\varepsilon_r \approx 5$ ,<sup>34</sup> and  $t \approx 3$  nm in accordance with microscopy studies,<sup>35</sup> we deduce that, when  $w$  is in the order of 10  $\mu\text{m}$ , the characteristic frequency of our circuit model  $f_{RLC}=1/(LC)^{1/2} \approx 10^{12} \text{ s}^{-1}$ , which is close to the values of  $f_1$  reported in the literature (see Table II). Moreover,  $\varepsilon/t$  appears to scale with  $w$ . Considering the dependence on  $\delta$  and  $w$  of the elements  $R$ ,  $L$  and  $C$  we obtain  $f_{RLC} \approx G(w)^{1/2}$ , where  $G$  is a function exclusively dependent on  $\delta$ . On the other hand, combining the expressions of  $V_1$  and  $\bar{\tau}$ ,  $f_1=K/w(\varepsilon/t)^{1/2}$  where  $K$  is again a function exclusively dependent on  $\delta$ . Comparing these expressions, both resonant frequencies present similar values if the product  $w \times \varepsilon/t$  depends only on  $\delta$ . In our experiments where the thickness of the samples was always fixed to 500  $\text{\AA}$ , we effectively verify this scaling law, as can be seen in Table II. We have also quoted data reported by other authors who have followed the same procedure to deduce  $\bar{\tau}$  and  $\varepsilon/t$  from Fiske and flux flow resonances. According to our discussion a comparison in terms of  $\varepsilon/t$  is only strictly possible for junctions of the same width and thickness, which is not the case.

We conclude that a simple circuit model can explain the dependencies of the electromagnetic parameters on the geometry of the junction. Each element of the circuit has a clear physical meaning: the dielectric response of the material reveals a peculiar barrier microstructure that can be described in the context of the filamentary model, i.e., a disordered dielectric medium with a high density of superconducting filaments taken into account in an inductive behavior. Strictly, the kinetic inductance of the junction should depend on the number of superconducting filaments, so on the junction width. However, data in Table II reveals that the electromagnetic parameters  $\bar{\tau}$  and  $\varepsilon/t$  are only slightly dependent on properties directly related with the filament distribution such as  $R_N$  and  $I_C$  as discussed previously. For instance, junctions with similar  $R_N$  (4.5  $\Omega$ ) and widths of 30  $\mu\text{m}$  and 10  $\mu\text{m}$  show values for  $\varepsilon/t$  of 2.6 and 8.8  $\text{nm}^{-1}$ , respectively. Junctions with different  $R_N$  and same  $w$  present very similar values of  $\varepsilon/t$ . In this sense we believe that considering  $L$  similar for all our junction widths is a good approach, and depends mainly on  $\delta$ .

## B. He<sup>+</sup> irradiation effects

As a possible attempt to modify the microstructure and the transport properties of the barrier, we have undertaken a study of the effect of light ion irradiation at low energies on our samples. The results obtained on a 2  $\mu\text{m}$ -wide junction are shown in Fig. 1, where  $I_C(B)$ , first Fiske step intensity and  $I_C(T)$  can be compared before and after irradiation. For small junctions, the dose was fixed at  $5 \times 10^{13} \text{ cm}^{-2}$ . After the implantation process a decrease in the critical temperature from 89 to 78 K can be observed. Bare GBJ-free patterned YBCO microbridges with the same width and irradiated with the same dose show very similar decrease in  $T_C$ , confirming that damaging of the electrodes is responsible for changes in  $T_C$ . In contrast, the reduction of  $R_N$  from 17.5 to 14.5  $\Omega$  along with the increase of  $I_C(T)$  reveals the surprising conclusion of a stronger coupling behavior of the irradiated boundary. Moreover, critical currents always decrease after irradiation in epitaxial GBJ-free films, so rises of  $I_C$  in the bicrystalline films should be interpreted in terms of alterations in the barrier structure, at least qualitatively. We can also observe in Fig. 1(b) an enhancement in the amplitude of the first Fiske step after irradiation, in good agreement with the increase of  $I_C$ . Ion irradiation also induces a shift in the position of these resonances that corresponds to an increase in the Swihart velocity from  $1.8 \times 10^6$  to  $2.0 \times 10^6$  m/s and a decrease in the  $\varepsilon/t$  value from 33.6 to 23  $\text{nm}^{-1}$ . The results are in agreement with photoexcitation experiments<sup>8</sup> where a decrease in the ratio  $\varepsilon/t$  is a consequence of a reduction in the normal resistance. In our experiments the shape of the  $I_C(B)$  pattern is not modified by irradiation at any temperature indicating no significant changes in the current distribution. The width of the oscillations decreases due to the increase in the value of  $\lambda_L$  of the electrodes (i.e., a decrease of  $T_C$ ). Comparing the flux density expression before and after implantation, and considering that  $F$  is unchanged, the relation  $\lambda_{\text{after}}=(\Delta B_{\text{before}}/\Delta B_{\text{after}})\lambda_{\text{before}}$  allows to determine the change in  $\lambda$ , and thus  $\lambda_L$ , and so the relation  $\varepsilon/t$  after irradiation:  $\lambda_{\text{after}}=479 \text{ nm}$  at 15 K. This means a value of  $\lambda_L=152 \text{ nm}$ . Interestingly, the modified values of the penetration depth of epitaxial YBCO in the electrodes damaged by the implantation process can be assigned for each dose following this procedure. The enhancement observed in the transparency of the barrier can be interpreted assuming that implantation promotes a partial structural rearrangement preferentially in the more disordered region that is concentrated in the barrier. This idea is in the same line as earlier electromigration experiments in YBCO microbridges containing grain boundaries where weak-link properties can be improved.<sup>6</sup> The critical current can also be enhanced when samples are annealed in ozone, diffusion and oxygen doping is favored into the grain boundary.<sup>17</sup> Experiments performed on grain boundaries in other materials show that diffusion processes can also be activated by electron irradiation.<sup>36</sup>

From our studies we conclude that at the higher doses ( $5 \times 10^{14} \text{ cm}^{-2}$ ) we always observe a degradation of the superconductivity of the electrodes and the coupling of the barrier. However, the shape of  $I_C(B)$  is always maintained, indicating again that the current distribution is not remarkably altered. Only changes in the behavior of the junction

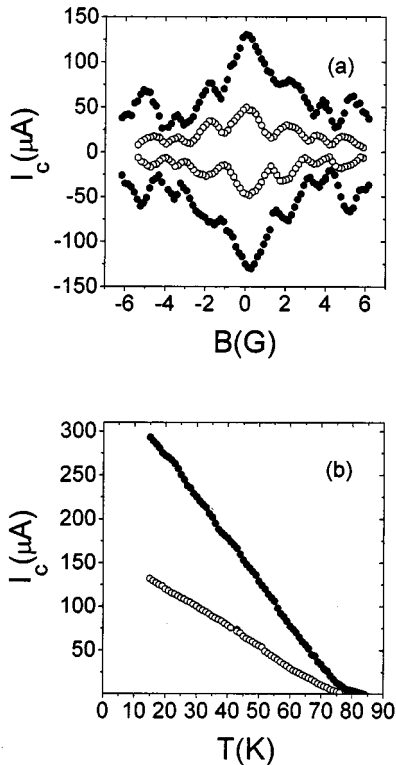


FIG. 2. Magnetic field dependence at 50 K (a) and temperature dependence (b) of the critical current before (black dots) and after irradiation (white dots). The dose is  $8 \times 10^{13} \text{ cm}^{-2}$  and the junction width is  $4 \text{ } \mu\text{m}$ . The symmetry relation  $I_C^+(+B) = -I_C^-(-B)$  is obeyed.

from long to small regime can drastically modify the modulation of the  $I_C(B)$  curve to a Fraunhofer diffractionlike pattern. As an example, we show in Fig. 2(a) the modification of the diffraction pattern at 50 K of a  $4 \text{ } \mu\text{m}$ -wide junction after an irradiation process with dose  $8 \times 10^{13} \text{ cm}^{-2}$ . The critical current decreases as shown in Fig. 2(b) and  $R_N$  rises from 7 to  $13.5 \text{ } \Omega$ , corresponding to a Swihart velocity change from  $2.6 \times 10^6$  to  $2.2 \times 10^6 \text{ m/s}$  and an increase of the value of the ratio  $\varepsilon/t$  from 16.1 to  $18.6 \text{ nm}^{-1}$  at 20 K. The critical temperature decreases from 88 to 75 K and the value of  $\lambda_L$  increases up to 156 nm at 20 K. In this case irradiation has induced a change of the junction parameters such that the small junction behavior is approached: for instance at 50 K the ratio  $w/\lambda_J$  varies from 6 to 4 using the expression  $\lambda_J = (\phi_0/4\pi\mu_0 J_C \lambda)^{1/2}$  for the Josephson penetration depth.<sup>29</sup>

The improvement of weak-link properties only occurs when the  $T_C$  of the electrode is not severely degraded by irradiation. In any case  $I_C R_N$  product always decreases as a consequence of irradiation, in agreement with the degradation of  $T_C$  of the electrodes. 65% of our irradiated microbridges (small and large junctions) showed an increase of  $I_C$  for the lowest doses. This percentage indicates the degree of reproducibility of our experiments, but we believe that it may be ameliorated by finely tuning the correct dose for each junction. A systematic study of the dose influence on the  $I_C(B, T)$  curves,  $I_C R_N$  product, excess current, Fiske and flux flow resonances will be published later.

#### IV. SUMMARY

Summarizing, despite the structural complexity of GBJ's we have shown that some important conclusions can be extracted from the analysis of the transport and electromagnetic parameters. We found that the value of  $I_C$  is mainly dependent on  $R_N$  and not on the width of the junction. This result has been explained assuming a random distribution of superconducting filaments in the grain boundary. Considering  $t$  similar in all the junctions,  $\varepsilon$  deduced from Fiske resonances is found to depend mainly on  $w$ . Varying  $w$  we obtain  $\varepsilon(f_1)$  relations that can be explained as a resonant behavior in the dielectric response of the barrier: a simple circuit model accounts for this mechanism if the kinetic inductance is taken into account.

We have demonstrated the potential of light ion implantation as a tool to controllably modify these parameters, without remarkable alteration of critical current spatial distribution in the junction. The most interesting result is the possibility to increase the critical current of GBJ's although the  $T_C$  of the electrodes is degraded. This result suggests that an atomic rearrangement in the barrier induced by ion tracks can take place, and may give complementary information about the nature of the microstructure of the junctions. This opens new possibilities to tailor *a posteriori* barrier performances and hence devices based on Josephson junctions.

#### ACKNOWLEDGMENTS

The authors would like to thank C. A. I. de Implantación Iónica from the Universidad Complutense in Madrid for assistance with ion implantation and lithography facilities. Financial support from CICYT Grant No. MAT97-0675 is acknowledged.

<sup>1</sup>S. Pagano and A. Barone, Supercond. Sci. Technol. **10**, 904 (1997).

<sup>2</sup>N. F. Heinig, R. D. Redwing, I. Fei Tsu, A. Gurevich, J. E. Nordman, S. E. Babcock, and D. C. Larbalestier, Appl. Phys. Lett. **69**, 577 (1996).

<sup>3</sup>D. Dimos, P. Chaudhari, J. Mannhart, and F. K. LeGoues, Phys. Rev. Lett. **61**, 219 (1988).

<sup>4</sup>T. Ogawa and M. Koyanagi, Appl. Phys. Lett. **70**, 2183 (1997).

<sup>5</sup>N. D. Browning, J. P. Buban, P. D. Nellist, D. P. Norton, M. F.

Chisholm, and S. J. Pennycook, Physica C **294**, 183 (1998).

<sup>6</sup>B. H. Moeckly, D. K. Lathrop, and R. A. Buhrman, Phys. Rev. B **47**, 400 (1993).

<sup>7</sup>E. A. Early, R. L. Steiner, A. F. Clark, and K. Char, Phys. Rev. B **50**, 9409 (1994).

<sup>8</sup>J. Elly, M. G. Medici, A. Gilabert, F. Schmidl, P. Siedel, A. Hoffmann, and Ivan K. Schuller, Phys. Rev. B **56**, R8507 (1997).

<sup>9</sup>I-Fei Tsu, Jyh-Lih Wang, D. L. Kaiser, and S. E. Babcock,

- Physica C **306**, 163 (1998).
- <sup>10</sup>R. Dimos, P. Chaudhari, and J. Mannhart, Phys. Rev. B **41**, 4038 (1990).
- <sup>11</sup>M. F. Chisholm and J. Pennycook, Nature (London) **351**, 47 (1991).
- <sup>12</sup>M. B. Field, D. C. Larbalestier, A. Parikh, and K. Salama, Physica C **280**, 221 (1997).
- <sup>13</sup>O. M. Froehlich, H. Schulze, A. Beck, B. Mayer, L. Alff, R. Gross, and R. P. Huebener, Appl. Phys. Lett. **66**, 2289 (1995).
- <sup>14</sup>O. Neshor and E. N. Ribak, Appl. Phys. Lett. **71**, 1249 (1997).
- <sup>15</sup>R. Fehrenbacher, V. B. Geshkenbein, and Gianni Blatter, Phys. Rev. B **45**, 5450 (1992).
- <sup>16</sup>R. Gross, P. Chaudhari, M. Kawasaki, and A. Gupta, Phys. Rev. B **42**, 10 735 (1990).
- <sup>17</sup>M. Kawasaki, P. Chaudhari, and A. Gupta, Phys. Rev. Lett. **68**, 1065 (1992).
- <sup>18</sup>A. Schmehl, B. Goetz, R. R. Schulz, C. W. Schneider, H. Bielefeldt, H. Hilgenkamp, and J. Mannhart, Europhys. Lett. **47**, 110 (1999).
- <sup>19</sup>C. W. Schneider, R. R. Schulz, B. Goetz, A. Schmehl, H. Bielefeldt, H. Hilgenkamp, and J. Mannhart, Appl. Phys. Lett. **75**, 850 (1999).
- <sup>20</sup>F. Tafuri, S. Shoklor, B. Nadgorry, M. Gurvitch, F. Lombardi, and A. Di Chiara, Appl. Phys. Lett. **71**, 125 (1997); F. Tafuri, B. Nadgorny, S. Shoklor, M. Gurvitch, F. Lombardi, F. Carillo, A. Di Chiara, and E. Sarnelli, Phys. Rev. B **57**, 14 076 (1998).
- <sup>21</sup>E. M. Jackson, B. D. Weaver, and G. P. Summers, Appl. Phys. Lett. **71**, 273 (1997).
- <sup>22</sup>U. Poppe, N. Klein, U. Dahne, H. Soltner, C. L. Jia, B. Kabius, K. Urban, A. Lubig, K. Schmidt, S. Henger, S. Orbach, S. Müller, and H. Piel, J. Appl. Phys. **71**, 5572 (1995).
- <sup>23</sup>T. Amien, L. Shultz, B. Kabius, and K. Urban, Phys. Rev. B **51**, 6792 (1995).
- <sup>24</sup>V. Ambegaokar and B. L. Halperin, Phys. Rev. Lett. **22**, 1364 (1969).
- <sup>25</sup>R. Gross, P. Chaudhari, D. Dimos, A. Gupta, and G. Koren, Phys. Rev. Lett. **64**, 228 (1990).
- <sup>26</sup>Peter A. Rosenthal, M. R. Beasley, K. Char, M. S. Colclough, and G. Zaharchuk, Appl. Phys. Lett. **59**, 3482 (1991).
- <sup>27</sup>Y. M. Zhang, D. Winkler, P. A. Nilsson, and T. Claeson, Phys. Rev. B **51**, 8684 (1995).
- <sup>28</sup>A. Barone and G. Paterno, *Physics and Applications of the Josephson Effect* (Wiley, New York, 1982).
- <sup>29</sup>D. Winkler, Y. M. Zhang, P. A. Nilsson, E. A. Stepanov, and T. Claeson, Phys. Rev. Lett. **72**, 1260 (1994).
- <sup>30</sup>M. D. Fiske, Rev. Mod. Phys. **36**, 221 (1964).
- <sup>31</sup>T. J. Rajeevakumar, Appl. Phys. Lett. **39**, 439 (1981).
- <sup>32</sup>H. Hilgenkamp, J. Mannhart, and B. Mayer, Phys. Rev. B **53**, 14 586 (1996).
- <sup>33</sup>S. K. Tolpygo and M. Gurvitch, Appl. Phys. Lett. **69**, 3914 (1996).
- <sup>34</sup>J. Humlicek, J. Kircher, H. U. Habermeier, M. Cardona, and A. Roseler, Physica C **190**, 383 (1992).
- <sup>35</sup>J. W. Seo, B. Kabius, U. Dahne, A. Scholen, and K. Urban, Physica C **245**, 25 (1995).
- <sup>36</sup>Tokushi Kizuka, Motoaki Iijima, and Nobuo Tanaka, Philos. Mag. A **77**, 413 (1998).